ISBN: 978-3-95450-253-0 ISSN: 2673-5571 doi:10.18429/JACoW-HB2023-MOA3I1

BEAM DYNAMICS CHALLENGES IN THE DESIGN OF THE ELECTRON-ION COLLIDER*

Y. Luo†, M. Blaskiewicz, A. Blednykh, D. Marx, C. Montag, V. Ptitsyn, V. Ranjbar, S. Verdú-Andrés, E. Wang, F. Willeke, Brookhaven National Laboratory, Upton, NY, USA
S. Nagaitsev, Thomas Jefferson National Accelerator Facility, Newport News, VA, USA

Abstract

The Electron-Ion Collider (EIC), which will be constructed at Brookhaven National Laboratory, will collide polarized high-energy electron beams with hadron beams, achieving luminosities up to $1 \times 10^{34}\text{cm}^{-2}\text{s}^{-1}$ in the center-of-mass energy range of 20-140 GeV. To achieve such high luminosity, we adopt high bunch intensities for both beams, small and flat transverse beam sizes at the interaction point, a large crossing angle of 25 mrad, and a novel strong hadron cooling in the Hadron Storage Ring to counteract intra-beam scattering (IBS) at the collision energies. In this article, we will review the beam dynamics challenges in the design of the EIC, particularly the beam-beam interaction, impedance budget and instabilities, polarization maintenance, and dynamic aperture. We will also briefly mention some technical challenges associated with beam dynamics in the design of EIC, such as strong hadron cooling, noises of crab cavities and power supply current ripples.

INTRODUCTION

The Electron-Ion Collider (EIC) will be built at Brookhaven National Laboratory (BNL) in a full partnership between BNL and the Thomas Jefferson National Accelerator Facility (JLab). The EIC will uniquely address three profound questions about nucleons—neutrons and protons, and how they assemble to form the nuclei of atoms: 1) How does the mass of the nucleon arise? 2) How does the spin of the nucleon arise? 3) What are the emergent properties of dense systems of gluons? [1]

The storage ring-based design of the EIC meets or even exceeds the requirements referenced in the 2015 Long Range Plan for U.S. Nuclear Physics [2]: 1) Center-of-mass energy range from 20 to 100 GeV, upgradable to 140 GeV; 2) Ion beams from deuterons to the heaviest stable nuclei, 3) High luminosity, up to $1 \times 10^{34}\text{cm}^{-2}\text{s}^{-1}$ for electron-proton collisions; 4) Highly spin-polarized electron, proton, and light-ion beams, 5) An interaction region and integrated detector capable of nearly 100% kinematic coverage, with the capability of incorporating a second such interaction region as needed.

Figure 1 presents the schematic diagram of the EIC layout. The hadron storage ring (HSR) comprises arcs of the two superconducting Relativistic Heavy Ion Collider (RHIC) storage rings. An electron storage ring (ESR) will be installed in the existing RHIC tunnel, where it will provide beam collisions with the HSR hadron beam in up to two interaction regions (IRs). High polarized electron bunches will be provided to the ESR by a rapid-cycling synchrotron (RCS) in the same tunnel [3].

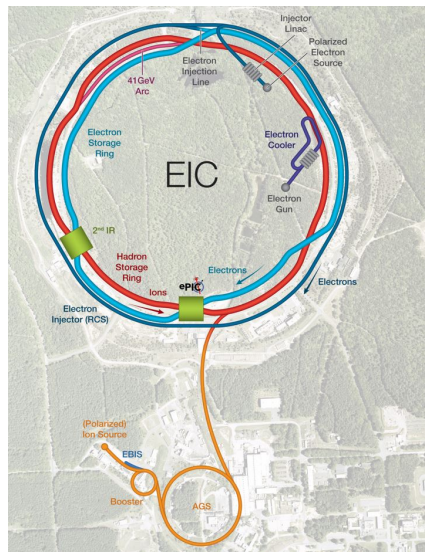

Figure 1: Schematic diagram of the EIC.

HIGHLIGHTS OF EIC DESIGN

The maximum luminosity in the EIC is limited by a range of factors. The primary factors are attainable beam-beam parameters (ξ_h, ξ_e), maximum beam divergences (σ_h', σ_e') at the interaction point (IP) defined by the interaction region magnet apertures and detector forward acceptance requirements, and maximum beam currents [1,4]. The luminosity can be written as

$$L = f_b \frac{\pi \gamma_h \gamma_e}{r_{0,h} r_{0,e}} (\xi_h \sigma_h')(\xi_e \sigma_e') \frac{(1+K)^2}{K} H \qquad (1)$$

where f_b is the bunch repetition rate, $\gamma_{h,e}$ are the relativistic factors of the respective beams, and $r_{0,h,e}$ are the classical radii of the electron and the hadron. $K = \sigma_y^*/\sigma_x^*$ is the aspect beam size ratio at the IP, where the beam sizes of electron and hadron beams are assumed fully matched. The factor H describes the luminosity modification due to the hourglass effect and crossing angle. For maximum luminosity one needs high beam-beam parameters, flat beams at the IP and as many bunches as allowed by average beam current limits or bunch spacing related limits.

For the EIC design, collision parameters of unequal species for each beam are chosen as if they would collide

* Work supported by the U.S. Department of Energy, Office of Science under contracts DE-SC0012704 and DE-AC05-06OR23177.
† yluo@bnl.gov

ISBN: 978-3-95450-253-0 ISSN: 2673-5571 doi:10.18429/JACoW-HB2023-MOA3I1

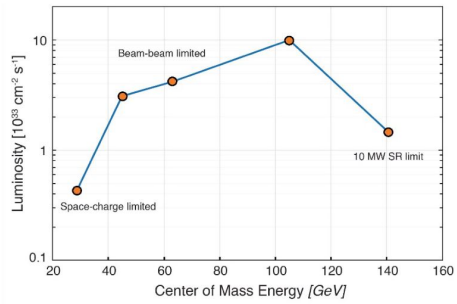

Figure 2: The design peak luminosity of electron-proton collisions versus the center-of-mass energy.

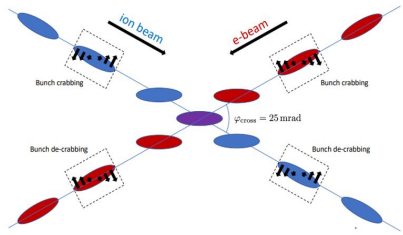

Figure 3: Schematic plot of crossing angle collision with crab cavities in the EIC.

with their own species. Hadron beam parameters differ from present RHIC by a smaller vertical emittance, 10 times more bunches, and 3 times more average beam current. Two hours IBS growth time requires hadron cooling at store. Flat beam is generated at injection energy with electron cooling. Electron beam parameters resemble a B-Factory: high beam current, large beam-beam tune shift of 0.1. High circulating beam currents, up to 1 A for protons and up to 2.5 A for electrons, requires considerable accelerator physics studies as well as accelerator system design to ensure the high beam current operation. Figure 2 shows the luminosity of electron-proton collisions versus the center-of-mass energy. Table 1 shows the design parameters for the highest luminosity collision mode with strong hadron cooling.

A large crossing angle of 25 mrad at the IP is required for the quick separation of colliding beams, allowing for more than 1000 bunches in each ring without the introduction of separator dipoles in the detector vicinity. Crab cavities are to be installed on both sides of the IR in both rings to compensate the geometric luminosity loss due to the large crossing angle. Figure 3 shows a sketch of the crossing angle collision with crab cavities in the EIC.

Flat beams with a transverse beam size ratio of about 11:1 at the IP are required for high luminosity. The electron beam naturally features this large ratio. Recently, we experimentally demonstrated an 11:1 transverse ratio in the RHIC with 100 GeV/nucleon gold ion beam with vertical stochastic cooling and fine decoupling [5]. We also demonstrated flat beam collisions with a beam-beam parameter of approximately 0.005. There is an experiment in preparation

Table 1: Key Beam Parameters for Collision Mode Between 10 GeV Electron and 275 GeV Proton Beams

Quantity	Unit	Proton	Electron
Beam energy	GeV	275	10
Bunch intensity	10^{11}	0.668	1.72
(β_x^*, β_y^*) at IP	cm	(80, 7.2)	(55, 5.6)
Beam sizes at IP	μm	(95, 8.5)	
Trans. emittances	nm	(11.3, 1.0)	(20.0, 1.3)
Bunch length	cm	6	0.7
Energy spread	10^{-4}	6.8	5.8
Peak Luminosity	$cm^{-2}s^{-1}$	1×10^{34}	

to obtain this emittance ratio at 26 GeV/nucleon and then accelerate it to 106 GeV/nucleon.

The HSR needs to operate over a wide energy range, for example, from 41 GeV to 275 GeV in the case of protons. The revolution time needs to be the same for all energies to keep hadrons and electrons in collision. Synchronization can be accomplished by changing the path length of hadron beam [6, 7]. For proton energies between 100 GeV and 275 GeV, this can be done by a radial shift of the beam orbit. For lower energies, the beam circulates in an inner arc as a shortcut.

To keep the ESR in one plane and to avoid vertical beam excursions at the IRs, the ESR plane is rotated by approximately 200 μrad around a line connecting IP6 and IP8. Vertical beam excursions may be detrimental to polarization. The tilted ESR plane equivalently introduces an $x - y$ axis rotation of about 4 mrad to both HSR and ESR before and after beam-beam interaction [8]. These rotation angles can be compensated together with the detector solenoid.

BEAM DYNAMICS CHALLENGES

Beam-Beam Interaction

There are several challenges for the EIC beam-beam interaction:

- Large beam-beam parameters: The maximum beam-beam parameters of about 0.1 in the ESR and 0.015 in the HSR are used for the EIC design. However, the combination of these parameters has never been experimentally demonstrated. The beam-beam parameter for the HERA-p is approximately 0.0014, which is about 10 times smaller than the maximum beam-beam parameter in the EIC design. The beam-beam parameter for HERA-e is about 0.12 with two experiments.
- Large crossing angle 25 mrad: Although a 22 mrad crossing angle was used in the lepton collider KEK-B, such a large crossing angle has never been used for a hadron collider. For the luminosity upgrade project of LHC, or HL-LHC, the crossing angle is about 0.5 mrad.
- Crab cavities in the both rings: A single crab cavity was used in KEK-B but it did not double its luminosity as planned. In the EIC design, the effects of the detector solenoid are not locally compensated near the IP. The combined effects from the detector solenoid and

ISBN: 978-3-95450-253-0 ISSN: 2673-5571 doi:10.18429/JACoW-HB2023-MOA3I1

the nearby crab cavities need to be carefully compensated [9, 10].

- Flat beam at the interaction point: A flatter beam at the IP will lead to a smaller dynamic aperture and a larger proton vertical beam size growth rate [11]. The ratio of the vertical to the horizontal beam sizes at the IP is 0.09 for the EIC, while it was 0.27 for the HERA. Flat beam also causes proton vertical emittance easily to grow due to machine noises.
- Synchro-betatron resonances: Synchro-betatron resonances have been observed in many EIC beam-beam simulation studies. This may be caused by the large crossing angle, large synchrotron tunes, and beam-beam interaction with flat beams. Mitigation methods include working point optimization and using second harmonic crab cavities in the HSR [12].
- Near-integer tunes for the electron beam: Near-integer tunes are chosen for the ESR to avoid overlapping of the design spin tune of 0.5. Because of the pinch effect with beam-beam interaction, electron beam sizes become smaller, yielding high luminosity. However, smaller electron beam sizes at IP increase the proton beam-beam parameter. Near-integer tunes also make it difficult for online optics controlling and correction [13].
- Combined effects with beam-beam: Beam-beam interplays with beam instability, noises from crab cavities and power supply current ripples, space charge effect, and polarization. Emittance mismatching, injection kicker errors during the electron bunch replacement needs further evaluation [14].

Currently, we are working on finalizing the EIC beam-beam related design parameters, determining tolerances for various optics imperfections and machine errors, and understanding the interplays between beam-beam and other effects.

Impedance Budget and Instabilities

Three different codes (GdfidL, CST, and ECHO3D) are employed for the impedance modelling of the EIC vacuum components in time domain and frequency domain. Good agreements have been reached among these codes in general. Iterations on the vacuum component design and impedance optimization for RCS, ESR, and HSR are in progress [15, 16].

The standard vacuum chamber for the ESR has an elliptical cross-section with an 80 mm full width and a 36 mm vertical full height. Each vacuum component undergoes several iterations in impedance optimization. Based on the electron energy, the orbit will be shifted relative to the vacuum chamber center due to the super-bends in the arcs. Beam-induced heating simulations were performed by the CST code. The obtained results are used for Finite Element Analysis (ANSYS) for thermal studies.

The HSR will re-use arcs of RHIC rings and some interaction regions. The transverse and longitudinal broadband impedances of RHIC had been measured by observing the tune shift as a function of the bunch intensity [17, 18]. The narrow band longitudinal impedance corresponds to the most dangerous mode from 197 MHz storage cavities. The transverse impedance corresponds to the most dangerous mode in the crab cavities.

The 4.5 K stainless steel beam pipe in the superconducting magnets and the cold mass interconnects of RHIC is not suitable for the EIC beams due to excessive resistive wall heating and electron cloud buildup. Solutions include beam screens inside existing SC magnet bores with active cooling and redesign of the inter-connections [19]. Work is ongoing to determine the optimal randomized pattern of pumping slots in the screen that mitigates high-Q narrow-band resonances. The low SEY required to suppress e-cloud buildup motivates the study of scrubbing beams and mitigation strategies like hybrid filling schemes

Coherent instabilities have been studied using a modified version of TRANFT [20]. The code has evolved to simulate both single-bunch and coupled-bunch instabilities by typically considering a few bunches and assuming a uniform fill. The code tracks all three dimensions. When beam-beam is used both transverse dimensions are subjected to the beam-beam force. The longitudinal and one transverse dimension are subjected to wakefields.

In ESR, the single-bunch instability threshold is above the requirement for stable operation [15]. Many components require water cooling due to beam-induced heating. The beam-beam interaction provides a large tune spread to Landau damp the transverse coupled-bunch instability and ion instability [21]. A longitudinal damper may be needed in the presence of longitudinal coupled bunch instability. When we do vacuum scrubbing in the ESR, we will probably need a transverse damper and a longitudinal damper.

For HSR, transverse coupled-bunch instabilities are stabilized by weak-strong beam-beam tune spread. During injection and ramp, we might need a damper to damp instabilities driven by the crab cavity fundamental mode. In both ESR and HSR, there needs to be strong RF feedback on the crab cavities to reduce the apparent impedance [22].

For the RCS, using the ESR impedance, there is a fast head-tail instability at low energy. Various strategies are being explored to alleviate it. There are also concerns during bunch merging. Dampers are likely to be needed but considerations are preliminary.

We will continue to define the maximum allowed HOM and to calculate the impedance budget and hence the total wakefields/impedances for the three rings. Reduction of Landau damping from beam-beam tune spread is under investigation when coherent beam-beam motion is included.

Polarization

High beam polarization is essential for the EIC physics program. The goal for the average polarization at store is 70% for all these species: electrons, protons, and helions (3He+2 ions). Requirements for the longitudinal polarization of all polarized species at the IP are achieved through spin rotators on both sides of the IR in both ESR and HSR [23].

Highly polarized electron beams at 85% - 90% will be produced in a polarized electron source [24]. Preserving

ISBN: 978-3-95450-253-0 ISSN: 2673-5571 doi:10.18429/JACoW-HB2023-MOA3I1

polarization of electron bunches at acceleration in the RCS (from 400 MeV up to 18 GeV) was a big challenge. Applying full Snakes in this energy range is not realistic. A solution has been found in the form of a spin resonance-free lattice with high periodicity so that strong intrinsic and imperfection spin resonances are moved out of the acceleration energy range [25, 26]. Simulation studies confirmed that the spin resonance free lattice combined with sufficiently fast acceleration delivers 80% - 85% electron polarization to 18 GeV. The RMS vertical closed orbit needs to be less than 0.5 mm during acceleration.

The polarization of the electron bunches in the ESR immediately begins to decay due to Sokolov-Ternov and stochastic depolarization processes. In order to maintain high average polarization in the ESR, the electron bunches are replaced with fresh highly polarized bunches at intervals of a few minutes. The spin rotators may significantly enhance the process of stochastic depolarization and accelerate polarization decay. In order to keep depolarization in check so-called spin matching of solenoidal spin rotators has been accomplished [27]. Simulation results show that asymptotic polarization of 30% at 18 GeV, which delivers an average stored polarization of 70% with electron bunch replacement, was achievable [28, 29].

Other important questions to be answered during electron polarization studies are: 1) the generation and control of vertical emittance without compromising polarization, 2) the polarization with two interaction regions and two sets of the spin rotators, and 3) an optimal working point which satisfies both polarization and particle dynamics [4].

For hadron polarization, RHIC has been operating with polarized protons achieving up to 60% polarization at 255 GeV energy. Two Siberian Snakes per RHIC ring have been used to minimize polarization loss during acceleration when numerous spin resonances are encountered. Accelerating polarized helions in the HSR would present a bigger challenge than protons since the helion spin has stronger coupling to magnetic fields than the proton spin due to its larger value of anomalous magnetic factor G = -4.18. The solution is to add 4 more Snakes in the HSR to prevent polarization loss on the acceleration. The 4 more Snakes can be converted from the existing rotators in the RHIC Blue ring with different power supply polarities [23].

The current HSR lattice design dramatically changed the 6-folded symmetry of the RHIC Yellow ring, greatly impacting the intrinsic spin resonance structure. The amplitudes of most dangerous spin resonance lines are reduced. However, a 'forest' of spin resonance lines in the whole acceleration energy range has emerged, which may cause parametric spin resonances [30]. Simulation results show that proton polarization with 6 Snakes is maintained in the HSR for less than 1 mm.mrad emittance beam (nominal value is 0.5 mm.mrad rms). However, for helions polarization loss was observed with 0.5 mm.mrad emittance beam. Spin tracking studies are still ongoing as the HSR lattice design is still evolving.

Dynamic Aperture

EIC needs 20-25 nm horizontal emittance from 5 GeV to 18 GeV for optimum luminosity, but the equilibrium emittance in an electron storage ring depends on the beam energy. Betatron phase advance per FODO cell is the 'knob' used to adjust the emittance: 60-degree FODO cells for 10 GeV and 90-degree FODO cells for 18 GeV lattice. Super-bends are used for emittance generation below 10 GeV [1, 3].

The minimum requirement for the dynamic aperture of the ESR is 10 σ in all three dimensions. Most challenging case is the 18 GeV lattice with two interaction regions where the RMS momentum spread is 1.0×10^{-3}.

Due to the complexity of the IRs, which include crab cavities, spin rotators, and spectrometer dipoles, there is no suitable optics near the IP to install the conventional local chromaticity correction based on non-interleaved sextupole pairs. Therefore, correction of the final focus quadrupole introduced chromaticity is performed independently on each side of the IR using the adjacent arc sextupoles. We name this method as a semi-local correction scheme [31].

Different phase advances of FODO cells in the arcs require different sextupole groupings and power supply windings for chromatic correction and compensation of geometric resonance driving terms. For example, four sextupole families in each arcs are used for the 90-degree lattice at 18 GeV and six families for the 60-degree lattice at 5 GeV and 10 GeV.

After W-function correction, one remaining chromatic effect is a relatively large second-order dispersion caused mostly by dipoles outside of the arcs. To compensate this effect, we use 12 individually powered sextupoles at the ends of the arcs.

Magnet misalignment, strength errors, and non-linear field multipoles perturb the design optics, causing distortions of the beam orbit, dispersion, beta functions, x-y coupling, chromaticity, betatron tune, and excitation of non-linear resonances. These effects must be carefully corrected before dynamic aperture tracking [32]. The dynamic aperture is most sensitive to field errors in the low-beta IR magnets, where β functions are very large. Figure 4 shows the momentum dynamics aperture after chromatic optimization for the 18 GeV ESR lattice with 2 IRs.

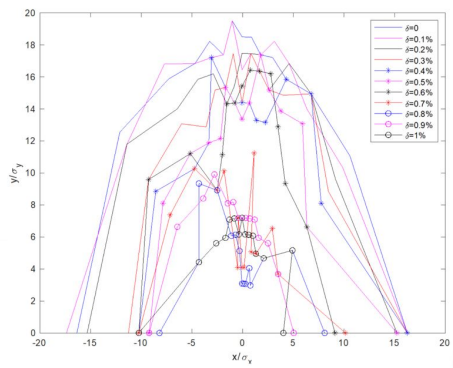

Figure 4: Dynamic aperture for the 18 GeV ESR lattice with two IRs.

ISBN: 978-3-95450-253-0 ISSN: 2673-5571 doi:10.18429/JACoW-HB2023-MOA3I1

For the HSR dynamic aperture, based on the operational experience at the RHIC, simulated DA with beam-beam and IR magnetic field errors should be larger than 5 σ to guarantee sufficient proton beam lifetime. For the HSR lattice with 1 IR, second order chromaticities are below 800 with two families of chromatic sextupoles. Further chromatic correction with more sextupole families is possible if needed.

10^6 turn dynamic apertures are calculated for protons at 275 GeV with $(dp/p_0) = 3(dp/p_0)_{rms}$, or 18×10^{-4}. 40 seeds of IR errors had been used for each tracking condition. Preliminary results show that with 1 unit of IR field errors, DA is more than 6 σ with beam-beam and 197 MHz crab cavities. Second harmonic crab cavities with 394 MHz are required to limit dynamic aperture reduction due to crab crossing to 1-2 σ, thus relaxing IR magnet tolerances [33].

We are continuing to work on the tolerances of IR magnetic field errors, especially for large physical aperture IR magnets. For this purpose, we are building a complete HSR tracking model to include all known linear and nonlinear optics and machine errors and their corrections.

TECHNICAL CHALLENGES

Strong Hadron Cooling

At the proton store energies, the IBS longitudinal and transverse (horizontal) growth time is 2-3 hours. Beam-beam linked growth time (vertical) is greater than 5 hours. The cooling time shall be equal to or less than the diffusion growth from all sources. The integrated luminosity with cooling is 10 times larger than without strong hadron cooling. Baseline for high energy hadron cooling is coherent electron cooling approach with a bandwidth range raised from GHz to tens of THz. Significant progress had been made on the EIC strong hadron cooling design [34–36]. Another scenario is storage ring cooler [37–41]. Its feasibility studies progress well, too. Final decision on which method to adopt for strong hadron cooling for the EIC will be made next year.

Crab Cavity Noises

Emittance growth due to amplitude and phase noises of crab cavities had been analytically estimated and experimentally measured at CERN [42, 43]. We used a weak-strong beam-beam model and element-by-element tracking to estimate the emittance growth from crab cavity noises [44, 45]. We confirmed the horizontal growth rate predicted by analytical calculation. Additionally, we observed vertical emittance growth with both phase noises and beam-beam interaction. To have proton vertical emittance growth rate less than 20%hour in both transverse planes, we need to have the RMS phase noise not more than 1 μrad, which is beyond the state-of-art of RF design. Countermeasures including RF low-level phase feedback, fast one-turn feedback, and high precision pickup 1 μm are all under investigation.

Power Supplies Current Ripples

Power supply current ripples, especially those from the main dipoles of the ESR, will introduce orbit oscillations at the IP, causing a sizeable proton emittance growth through beam-beam interaction. Weak-strong beam-beam simulation shows that to have proton beam size growth less than 10%/hour, orbit oscillation at the IP should be less than 2.5% $\sigma_{x,y}$ for the low frequency band (< 8 kHz), and less than $10^{-4}\sigma_{x,y}$ for the high frequency band [46]. The tolerance of dipole power supply current ripples at low frequency band is about 0.5-1.5 ppm depending on the magnets. The high-frequency ripples is less worrisome due to very significant eddy current shielding. We are continuing working on the conversion from the field ripple tolerance to the power supply current tolerance [47].

Low Field at RCS Injection Energy

The dipole field in the RCS is about 57 Gauss at injection energy 400 MeV, and 2.5 kGauss at the highest energy 18 GeV, with a large ratio of maximum to minimum fields 45. RCS beam spends its longest period of time (about 200 ms) at 1 GeV where bunch merging takes place. The dipole field at 1 GeV is 140 Gauss which is still quite low. Another concern is that eddy currents during power supply current ramp induce significant multipoles in the dipoles, potentially reducing dynamic aperture and deteriorating beam quality. RCS magnet R&D program started recently to measure low-field behavior, repeatability, hysteresis and to measure the stray field in the RHIC tunnel.

Longitudinal Emittance Preservation in RCS

RCS cycling rate is 1 Hz to replace ESR electron bunches to maintain high average polarization 70% during collision. 4->1 bunch merging takes place at beam energy 1 GeV. Four electron bunches with 7 nC/bunch merge to one bunch with 28 nC. Simulation results show that the RMS longitudinal emittance is $\sigma_E \times \sigma_t = 2.5 \times 10^{-4}$ eVs after bunch merging. The equilibrium RMS emittances in the ESR are 8×10^{-5} eVs at 5 GeV, 1.4×10^{-4} eV-s at 10 GeV, and 5.9×10^{-4} eVs at 18 GeV. Numerical simulations are onging to examine its impacts on dynamic aperture and beam-beam performance with synchrotron radiation damping in the ESR.

SUMMARY

The EIC with high luminosity and high polarization in a wide center-of-mass energy range will be a unique facility to study the contribution of quarks and gluons to nucleon spin and mass. In this article, we presented the beam dynamics challenges in the EIC design. We have made progress on the majority of accelerator physics topics. Crab cavity noise and feedback requirements are under further investigation. Final decision on which method to adopt for strong hadron cooling for the EIC will be made next year.

REFERENCES

[1] J. Beebe-Wang *et al.*, "Electron-Ion Collider: conceptual design report", Brookhaven National Laboratory, Jefferson

ISBN: 978-3-95450-253-0 ISSN: 2673-5571 doi:10.18429/JACoW-HB2023-MOA3I1

Lab, 2021. https://www.bnl.gov/EC/files/EIC_CDR_Final.pdf

[2] A. Aprahamian *et al.*, "Reaching for the horizon: the 2015 long range plan for nu- clear science." DOE/NSF Nuclear Science Advisory Panel (NSAC) Report, 2015.

[3] C. Montag *et al.*, "Design status of the Electron-Ion Collider", in *Proc. IPAC'23*, Venice, Italy, May 2023, pp. 136–139. doi:10.18429/JACoW-IPAC2023-MOPA049

[4] V. Ptitsyn, "Accelerator physics challenges for EIC", in *Proc. IPAC'23*, Venice, Italy, May 2023, pp. 2621–2626. doi:10.18429/JACoW-IPAC2023-WEZG1

[5] Y. Luo *et al.*, "Fine decoupling test and simulation study to maintain a large transverse emittance ratio in hadron storage rings", in *Proc. IPAC'22*, Bangkok, Thailand, Jun. 2022, pp. 1935–1938. doi:10.18429/JACoW-IPAC2022-WEPOPT039

[6] S. Peggs *et al.*, "Large radial shifts in the EIC Hadron Storage Ring", in *Proc. IPAC'21*, Campinas, Brazil, May 2021, pp. 1443–1446. doi:10.18429/JACoW-IPAC2021-TUPAB042

[7] J. Berg *et al.*, "Synchronizing the timing of the electron and hadron storage rings in the Electron-Ion Collider", in *Proc. IPAC'23*, Venice, Italy, May 2023, pp. 906–908. doi:10.18429/JACoW-IPAC2023-MOPL157

[8] D. Xu *et al.*, "Beam-beam interaction for tilted storage rings", in *Proc. IPAC'22*, Bangkok, Thailand, Jun. 2022, pp. 1968–1971. doi:10.18429/JACoW-IPAC2022-WEPOPT049

[9] B. R. Gamage *et al.*, "Detector solenoid compensation for the Electron-Ion Collider", in *Proc. IPAC'21*, Campinas, Brazil, May 2021, pp. 1439–1442. doi:10.18429/JACoW-IPAC2021-TUPAB041

[10] D. Xu and Y. Luo, "Detector solenoid compensation in the EIC Electron Storage Ring", in *Proc. IPAC'22*, Bangkok, Thailand, Jun. 2022, pp. 1972–1975. doi:10.18429/JACoW-IPAC2022-WEPOPT050

[11] Y. Luo *et al.*, "Beam-beam related design parameter optimization for the Electron-Ion Collider", in *Proc. IPAC'21*, Campinas, Brazil, May 2021, pp. 3808–3811. doi:10.18429/JACoW-IPAC2021-THPAB028

[12] D. Xu, Y. Hao, Y. Luo, and J. Qiang, "Synchrobetatron resonance of crab crossing scheme with large crossing angle and finite bunch length", *Phys. Rev. Accel. Beams*, vol. 24, p. 041002, 2021. doi:10.1103/PhysRevAccelBeams.24.041002

[13] Y. Luo *et al.*, "Optimizing the design tunes of the electron storage ring of the Electron-Ion Collider", in *Proc. IPAC'23*, Venice, Italy, May 2023, pp. 128–131. doi:10.18429/JACoW-IPAC2023-MOPA047

[14] J. Qiang *et al.*, "Transient beam-beam effect during electron bunch replacement in the EIC", in *Proc. IPAC'21*, Campinas, Brazil, May 2021, pp. 3228–3231. doi:10.18429/JACoW-IPAC2021-WEPAB252

[15] A. Blednykh *et al.*, "An overview of the collective effects and impedance calculation for the EIC", in *Proc. IPAC'21*, Campinas, Brazil, May 2021, pp. 4266–4269. doi:10.18429/JACoW-IPAC2021-THPAB238

[16] A. Blednykh *et al.*, "Impedance optimization of the EIC interaction region vacuum chamber", in *Proc. IPAC'21*, Campinas, Brazil, May 2021, pp. 4270–4273. doi:10.18429/JACoW-IPAC2021-THPAB239

[17] N. Biancacci *et al.*, "Transverse impedance measurement in RHIC and the AGS", in *Proc. IPAC'14*, Dresden, Germany, Jun. 2014, pp. 1730–1732. doi:10.18429/JACoW-IPAC2014-TUPRI071

[18] M. Blaskiewicz, J. M. Brennan, and K. Mernick, "Longitudinal impedance of RHIC", in *Proc. IPAC'15*, Richmond, VA, USA, May 2015, pp. 746–747. doi:10.18429/JACoW-IPAC2015-MOPMN020

[19] S. Verdú-Andrés *et al.*, "A beam screen to prepare the RHIC vacuum chamber for EIC hadron beams: conceptual design and requirements", in *Proc. IPAC'21*, Campinas, Brazil, May 2021, pp. 2066–2069. doi:10.18429/JACoW-IPAC2021-TUPAB260

[20] M. Blaskiewicz, "A multipurpose coherent instability simulation code", in *Proc. PAC'07*, Albuquerque, NM, USA, Jun. 2007, paper THPAS090, pp. 3690–3692.

[21] M. Blaskiewicz, "Beam-beam damping of the ion instability", in *Proc. NAPAC'19*, Lansing, MI, USA, Sep. 2019, pp. 391–394. doi:10.18429/JACoW-NAPAC2019-TUPLM11

[22] M. Blaskiewicz, "Instabilities driven by the fundamental crabbing mode", Brookhaven National Lab., Upton, NY, USA, Tech. Rep. BNL-222221-2021-TECH, 2021.

[23] V. Ptitsyn and J. S. Berg, "EIC hadron spin rotators", in *Proc. IPAC'22*, Bangkok, Thailand, Jun. 2022, pp. 1734–1736. doi:10.18429/JACoW-IPAC2022-WEPOST020

[24] E. Wang, O. Rahman, J. Skaritka, W. Liu, J. Biswas, C. Degen, P. Inacker, R. Lambiase, and M. Paniccia, "High voltage dc gun for high intensity polarized electron source", *Phys. Rev. Accel. Beams* vol. 25, p. 033401, 2022. doi:10.1103/PhysRevAccelBeams.25.033401

[25] V. H. Ranjbar *et al.*, "Spin resonance free electron ring injector", *Phys. Rev. Accel. Beams*, vol. 21, p. 111003, 2018. doi:10.1103/PhysRevAccelBeams.21.111003

[26] V. H. Ranjbar, F. Lin, H. Lovelace III, and F. Meot, "EIC rapid cycling synchrotron spin tracking update", in *Proc. IPAC'22*, Bangkok, Thailand, Jun. 2022, pp. 2439–2441. doi:10.18429/JACoW-IPAC2022-THPOST004

[27] V. Ptitsyn, C. Montag, and S. Tepikian, "Electron polarization in the eRHIC ring-ring design", in *Proc. IPAC'16*, Busan, Korea, May 2016, pp. 3403–3405. doi:10.18429/JACoW-IPAC2016-THPMR010

[28] E. Gianfelice-Wendt, private communications, 2023.

[29] M. Signorelli, G. Hoffstaetter, and V. Ptitsyn, "Electron polarization preservation in the EIC", in *Proc. IPAC'23*, Venice, Italy, May 2023, pp. 144–147. doi:10.18429/JACoW-IPAC2023-MOPA052

[30] V. Ranjbar, private communications, 2023.

[31] Y. Cai *et al.*, "Optimization of chromatic optics in the electron storage ring of the Electron-Ion Collider", *Phys. Rev. Accel. Beams*, vol. 25, p. 071001, 2022. doi:10.1103/PhysRevAccelBeams.25.071001

ISBN: 978-3-95450-253-0 ISSN: 2673-5571 doi:10.18429/JACoW-HB2023-MOA3I1

[32] Y. M. Nosochkov *et al.*, "Dynamic aperture of the EIC Electron Storage Ring", in *Proc. IPAC'22*, Bangkok, Thailand, Jun. 2022, pp. 1950–1953. doi:10.18429/JACoW-IPAC2022-WEPOPT043

[33] Y. Luo *et al.*, "Dynamic aperture evaluation for the Hadron Storage Ring in the Electron-Ion Collider", in *Proc. IPAC'21*, Campinas, Brazil, May 2021, pp. 3812–3814. doi:10.18429/JACoW-IPAC2021-THPAB029

[34] G. Stupakov and P. Baxevanis, "Microbunched electron cooling with amplification cascades", *Phys. Rev. Accel. Beams* 22, p. 034401, 2019. doi:10.1103/PhysRevAccelBeams.22.034401

[35] W. F. Bergan, P. Baxevanis, M. Blaskiewicz, G. Stupakov, and E. Wang, "Design of an MBEC cooler for the EIC", in *Proc. IPAC'21*, Campinas, Brazil, May 2021, pp. 1819–1822. doi:10.18429/JACoW-IPAC2021-TUPAB179

[36] E. Wang *et al.*, "Electron Ion Collider strong hadron cooling injector and ERL", in *Proc. LINAC'22*, Liverpool, UK, Aug.-Sep. 2022, pp. 7–12. doi:10.18429/JACoW-LINAC2022-MO2AA04

[37] D. Cline *et al.*, "High Energy Electron Beam Cooling to Improve the Luminosity and Lifetime in Colliding Beam Machines", in *Proc. PAC'79*, San Francisco, CA, USA, Mar. 1979, pp. 3472–3476.

[38] M. Gentner, R. Brinkmann, Y. Derbenev, D. Husmann, and C. Steier, "On the possibilities of electron cooling for HERA", *Nucl. Instrum. Methods Phys. Res. Sect. A* 424, 277 (1999).

[39] H. Zhao, J. Kewisch, M. Blaskiewicz, and A. Fedotov, "Ring-based electron cooler for high energy beam cooling", *Phys. Rev. Accel. Beams* 24, p. 043501, 2021. doi:10.1103/PhysRevAccelBeams.24.043501

[40] A. Blednykh, M. Blaskiewicz, R. Lindberg, and D. Zhou, "Microwave instability threshold from coherent wiggler radiation impedance in storage rings", *Phys. Rev. Accel. Beams* 26, p. 051002, 2023. doi:10.1103/PhysRevAccelBeams.26.051002

[41] A. Blednykh , D. Zhou , M. Blaskiewicz , R. Lindberg, " Microwave instability threshold from coherent wiggler radiation impedance in storage rings", in *Proc. IPAC'23*, Venice, Italy, May 2023, pp. 1085–1087. doi:10.18429/JACoW-IPAC2023-MOPM043

[42] P. Baudrenghien and T. Mastoridis, "Transverse emittance growth due to rf noise in the high-luminosity LHC crab cavities"*Phys. Rev. ST Accel. Beams* 18, p. 101001, 2015. doi:10.1103/PhysRevSTAB.18.101001

[43] R. Calaga *et al.* "First demonstration of the use of crab cavities on hadron beams", *Phys. Rev. Accel. Beams* 24, p. 062001, 2021. doi:10.1103/PhysRevAccelBeams.24.062001

[44] Y. Luo *et al.*, "6-D Element-by-Element Particle Tracking with Crab Cavity Phase Noise and Weak-Strong Beam-Beam Interaction for the Hadron Storage Ring of the Electron-Ion Collider", in *Proc. NAPAC'22*, Albuquerque, NM, USA, Aug. 2022, pp. 809–812. doi:10.18429/JACoW-NAPAC2022-WEPA75

[45] H. Huang *et al.*, "Quantifying effects of crab cavity RF phase noise on transverse emittance in EIC Hadron Storage Ring", in *Proc. IPAC'23*, Venice, Italy, May 2023, pp. 2399–2401. doi:10.18429/JACoW-IPAC2023-TUPM084

[46] D. Xu, M. Blaskiewicz, Y. Luo, D. Marx, C. Montag, and B. Podobedov, "Effect of electron orbit ripple on proton emittance growth in EIC", in *Proc. IPAC'23*, Venice, Italy, May 2023, pp. 108–111. doi:10.18429/JACoW-IPAC2023-MOPA039

[47] B. Podobedov, M. Blaskiewicz, Y. Luo, D. Marx, C. Montag, D. Xu, "ESR dipole power supply current ripple and noise specifications", BNL-224464-2023-TECH, 2023.